Noname manuscript No.
(will be inserted by the editor)

Throughput Improvement by Mode Selection in Hybrid Duplex Wireless Networks

Behnaz Mousavinasab ·
Amirhosein Hajihoseini Gazestani ·
Seyed Ali Ghorashi ·
Mohammad Shikh-Bahaei

Received: date / Accepted: date

Abstract Hybrid duplex wireless networks, use half duplex (HD) as well as full duplex (FD) modes to utilize the advantages of both technologies. This paper tries to determine the proportion of the network nodes that should be in HD or FD modes in such networks, to maximize the overall throughput of all FD and HD nodes. Here, by assuming imperfect self-interference cancellation (SIC) and using ALOHA protocol, the local optimum densities of FD, HD and idle nodes are obtained in a given time slot, using Karush–Kuhn–Tucker (KKT) conditions as well as stochastic geometry tool. We also obtain the sub-optimal value of the signal-to-interference ratio (SIR) threshold constrained by fixed node densities, using the steepest descent method in order to maximize the network throughput. The results show that in such networks, the proposed hybrid duplex mode selection scheme improves the level of throughput. The results also indicate the effect of imperfect SIC on reducing the throughput. Moreover, it is demonstrated that by choosing an optimal SIR threshold for mode selection process, the achievable throughput in such networks can increase by around 5%.

Keywords full duplex · hybrid duplex · mode selection · imperfect SIC · stochastic geometry · throughput

B. Mousavinasab and A. Hajihoseini Gazestani
Cognitive Telecommunication Research Group, Department of Electrical Engineering, Shahid Beheshti University G. C. Tehran, Iran

S. A. Ghorashi
Cognitive Telecommunication Research Group, Department of Electrical Engineering, Shahid Beheshti University G. C. Tehran, Iran and School of Architecture, Computing and Engineering, University of East London, London, UK.
E-mail: a_ghorashi@sbu.ac.ir

M. Shikh-Bahaei
Center for Telecommunications Research, King's College London, London, UK.

1 Introduction

Full duplex (FD) technology has attracted researchers due to its capability of sending and receiving information simultaneously, in the same frequency band. In this technology, the spectral efficiency can be doubled compared with traditional half duplex (HD) counterpart that uses time division duplex (TDD) or frequency division duplex (FDD) to send and receive information at different times or different frequencies, respectively [1], [2]. FD technology provides many advantages such as achieving high throughput gain, reducing collision probability, solving hidden terminal problem [3], and reducing end-to-end delay by sending and receiving simultaneously [4]. However, FD technology faces challenges such as self-interference (SI), link reliability reduction and packet loss incrementation compared to HD mode [3].

Self interference cancellation (SIC) architectures can be classified into passive and active suppression, and the active technique can be further divided into analog and digital cancellations [5]. Despite extensive studies performed on SIC architecture design, residual SI remains the primary challenge faced by FD nodes whose destructive influence on network performance is undeniable [6]. With the aim of improving network performance and to overcome aforementioned challenges, hybrid half/full-duplex systems are proposed [7] and [8] which allow a node to opportunistically switch optimally between the modes based on the network parameters.

1.1 Related Works

Researches have attempted to overcome FD challenges in recent years. For instance in [9] the impact of imperfect SIC in a FD Device-to-Device (D2D) communication has been investigated, where the authors proposed hybrid duplex designs to increase spectral efficiency and reduce outage probability of FD systems by employing an appropriate SIC factor. In addition, authors in [10] have investigated the secrecy performance of a downlink non-orthogonal multiple access (NOMA) system assisted by a multi-antenna FD relay with the presence of an eavesdropper and use beamforming at the multi-antenna relay to cancel its SI. Secure primary transmission by using a multi-antenna secondary FD NOMA relay in cognitive radio networks is proposed in [11]. Authors in [11] use FD relay to generate artificial noise to disrupt the eavesdropping while receiving the signal from primary transmitter, and they have shown that the secrecy rate of primary receiver in their scheme is better than the scheme without artificial noise (i.e., the scheme exploiting a HD relay). The interference alignment in small cell networks with FD self-backhauling equipped on each small base station has been investigated in [12]. Their result showed that FD self-backhauling scheme outperforms HD-enabled small cells scheme in terms of sum rate. [13] studies the secondary user throughput maximization problem, subject to a primary user delay constraint in a cooperative cognitive radio network. A comparison between FD and HD secondary user on the network performance has been also investigated in [13]. Their numerical results have shown that FD capability at the secondary user is not always better than the HD case and it can negatively affect the network stability region in some scenarios. In order to compare FD and HD gains in a large scale wireless network, a transmission capacity criterion has been introduced in [14], which is the maximum transmission throughput, subject to a constraint on the transmission outage probability of a typical link. This study is performed using the stochastic geometry tool and according to the Thomas cluster process model [15] for spatial distribution of FD and HD systems. In [14] the value of signal-to-interference-plus-noise ratio (SINR) threshold, as well as the optimal value of forward link density, that is available in the throughput equation, is calculated separately for FD-only and HD-only modes with the goal of maximizing the transmission capacity. It has been shown that at a low transmission rate, the transmission capacity for FD mode is greater than HD in contrast with the high transmission rate, when SI level is in FD mode. The maximum sum rate for heterogeneous multi-layer networks, in which users are equipped with FD and HD devices, is investigated in [16] by employing the stochastic geometry tool. For each user, the authors consider received power from its corresponding base station (BS) as the "mode selection" criterion. They stated that the reason for this policy in mode selection is that FD mode is not suitable for users whose level of signal strength is low due to the imperfect SIC. Also in [16] the optimal power threshold for changing the mode is calculated in order to maximize the sum rate. A joint resource allocation and transmission mode selection scheme to maximize the secrecy rate of multi channel cognitive radio networks in the presence of eavesdroppers is proposed in [17]. The result of proposed scheme in [17] in which each secondary user can select silent, HD or FD modes, showed that the proposed scheme dominates FD-only and HD-only scheme in terms of the secondary systems secrecy rate and energy efficiency. [18] studies cellular networks in which BSs have both FD and HD capabilities, but users only have HD devices, under the conditions of asymmetric traffic demand and imperfect SI suppression, using the stochastic geometry tool. In order to select the mode for maximizing the number of network-supported users, for each BS and in each time slot, the authors consider three modes: FD, HD uplink and HD downlink. Authors in [18] call this hybrid duplex scheme as XD mode and calculate the optimal times corresponding to each mode. Similar to [18], an X-duplex relay system with power allocation and the lower and upper bounds of the corresponding outage probability are investigated in [19]. Moreover, mode selection is performed in order to increase the number of discovered peers in a wireless peer discovery system, under imperfect SIC condition in [20]. [21] and [22] use a combination of FD and HD modes in relay-equipped systems in order to improve the throughput. In [22] authors improve the throughput of FD and HD modes in a relay-equipped system by controlling the duration of each transmission. In [23]-[26] the throughput is calculated using the stochastic geometry tool for heterogeneous multi-layer wireless networks, wireless ad-hoc networks, large-scale wireless networks and multi-cell networks, respectively. They also employed mode selection in order to improve the throughput level.

Authors in [24] maximize the throughput of a wireless ad-hoc network in which nodes are deployed randomly, under imperfect SIC condition. They concluded that by using the ALOHA protocol, the maximum throughput is achieved when all the concurrently transmitting nodes work in the same mode of FD or HD, depending on one defined condition. In contrast with [23] and [24] in which densities of FD and HD nodes are assumed to be predetermined, [25] and [26] seek to gain the ability of dynamic mode selection. In [25] the distance from the sender is considered as the mode selection criterion; if the distance of the communicating partner of a node is more than a predefined threshold value, the link should select HD mode, otherwise, FD mode is selected. The optimal value of this distance threshold in mode selection process is calculated with the goal of throughput maximization the throughput. In [25] it is also shown that usually the throughput for hybrid mode is better than both pure FD and pure HD modes. In [26] interference cancellation-enabled FD network with dynamic traffic request is studied, where BSs operate in different modes, i.e. FD, uplink HD and downlink HD and idle modes. [27] studies the secrecy throughput which is defined as the achievable rate of successful transmission per unit area under the required secrecy outage probabilities in a wireless network with a hybrid duplex receiver and randomly located eavesdroppers. Authors in [27] maximize the secrecy throughput by providing the optimal fraction of FD receivers. Hence, a part of researches such as [18] and [22] perform mode selection for a particular node, and determine how long a node should be in FD mode and how long it should be in HD mode. Some researches such as [28] make mode selection for a node during all transmission time based on system parameters, and others do this by specifying the density of FD and HD nodes in the network such as [24], [26] and [27]. Also, FD technology can be used for BS as mentioned in [18], relay node [19], users [16] and combination of them [29]. Some applications and implementation challenges of FD communication are reviewed in [30].

1.2 Main Contributions

Motivated by the above mentioned facts, in this paper we improve the overall throughput in wireless networks where nodes have both FD and HD capabilities. In the case of FD mode, the presence of SI results in throughput reduction. Therefore, unlike [24] in which all the concurrently transmitting nodes work in the same mode of FD or HD (depending on one defined condition), we obtain the local optimum values for densities of FD and HD nodes in a time slot subject to the total density constraint and under imperfect SIC using Karush–Kuhn–Tucker (KKT) conditions, in general and regardless of any condition. We also add the total density constraint to the problem discussed in [24] in order to consider practical assumptions. As explained in the previous subsection, the optimal value of criterion for changing the mode between FD and HD (i.e. SINR, power and distance) derived for wireless mesh [14], heterogeneous multi-layer [16] and large scale peer-to-peer wireless networks

[25] aims to maximize different objective functions. Similar to these mentioned works, we consider signal-to-interference ratio (SIR) as the success probability criterion, since the effect of additive noise is insignificant compared to interference [24]. Then, we calculate the sub-optimal value of SIR threshold under the condition that other network parameters are constant, in order to maximize the network throughput. Our numerical results indicate that the proposed hybrid duplex mode, outperforms both the pure HD and pure FD systems. Also, the undesirable effect of imperfect SIC on the throughput of a network with FD node is demonstrated. The contributions of this paper therefore, can be summarized as follows:

– Improving the throughput level in a mixed HD and FD wireless network by optimizing the density of FD and/or HD nodes in it,
– Solving the throughput maximization problem by optimizing the SIR threshold value.

The structure of this paper is as follows: Section 2 describes the model of a wireless network, using stochastic geometry. In Section 3 in order to optimize the throughput of the desired network, we calculate the local optimum values of the density of active nodes which are in FD and HD modes, based on the proposed mode selection scheme. Then, the sub-optimal SIR threshold value is computed. Section 4 analyzes numerical results of the proposed method and finally, conclusion is presented in Section 5.

2 System Model

We consider a wireless network whose links can be in HD mode with the probability of p_1, FD mode with the probability of p_2, and idle mode with the probability of p_3, where $p_1 + p_2 + p_3 = 1$. We assume that all nodes have a single antenna and are distributed according to the homogeneous Poisson point process (PPP), $\Phi = \{x_i\}$ with the density of λ in $\mathbb{R}^2$. We denote the location of the communication pairs associated with x_i, by $m(x_i)$ and assume that this pair has a constant distance R[1]. Therefore, $m(x_i)$ is a set of points on the circumference of a circle with center x_i and radius R in which the angles corresponding to these locations, are independent and distributed uniformly over $[0, 2\pi]$. Let $S(x_i)$ be a parameter to show the mode (i.e., HD, FD or idle mode) of each link including the communication pairs with positions x_i and $m(x_i)$. Then, we will have an independently marked PPP (IMPPP), $\hat{\Phi} = \{x_i, m(x_i), S(x_i)\}$ on $\mathbb{R}^2 \times \mathbb{R}^2 \times \{0, 1, 2\}$. The values of λp_i present the density of HD, FD and idle nodes for $S(x) = i$, $i \in \{1, 2, 3\}$, respectively. A link associated with x_i and $m(x_i)$ is called a typical link. An example for a realization of such a wireless network is illustrated in Fig. 1. Such system is

[1] The link distance R can also be random without affecting the main results such as success probabilities and maximal throughput, since we can always derive the results by first conditioning on R and then averaging over it [24].

practically applicable for the future wireless networks, such as D2D communications in vehicular networks [31], unmanned aerial vehicles communications [32] and cognitive radio ad hoc networks [33].

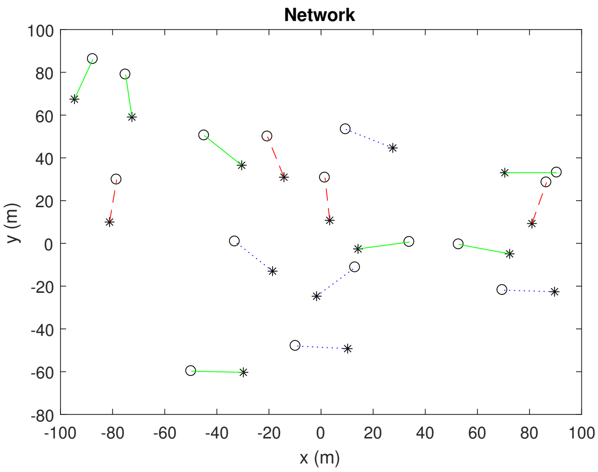

Fig. 1 An example of the class of wireless networks considered in this paper. The dashed lines indicate that the link is silent, the dotted lines mean that the link is in HD mode, and the solid lines mean that the link is in FD mode. The *s form Φ while the os form $m(\Phi)$.

In this paper, SIR is used in order to calculate the success probability and the success probability is defined as the probability of the SIR exceeds a threshold value [24]. When we deal with imperfect SIC in FD mode, the parameter β denotes the residual SI to the signal ratio. Thus, the SIR for a node y is calculated in two HD and FD modes in the following forms when the signal is sent from node x to y:

$$SIR_y^{HD} = \frac{P_{xy} K h_{xy} l(x,y)}{\sum\limits_{z \in \tilde{\Phi}/\{x\}} P_{zy} K h_{zy} l(z,y)} \tag{1}$$

$$SIR_y^{FD} = \frac{P_{xy} K h_{xy} l(x,y)}{\sum\limits_{z \in \tilde{\Phi}/\{x\}} P_{zy} K h_{zy} l(z,y) + \beta P_{yx}} \tag{2}$$

In this system, we assume identical transmit power for all nodes. Consequently, $P_{xy} = P_{yx} = P$ wherein P_{xy} and P_{yx} are the transmit powers when link xy is active. In addition, $\tilde{\Phi}$ is the set of transmitter nodes in a given time slot, and h_{xy} and h_{zy} are the fading power coefficients between the transmitter x and the receiver y and between the interferer z and the receiver y, respectively. K is a constant given as $K = G_{tx} G_{rx} (\frac{c_L}{4\pi f_c})^2$, G_{rx} and G_{tx} are the transmitter's and receiver's antenna gain, c_L is the speed of light, and f_c is the carrier frequency of the signal. Moreover, $l(x,y) = \|x-y\|^{-\alpha}$ is the path-loss function and $\alpha > 2$ is the path-loss exponent. In FD mode, the amount of residual SI, i.e. βP_{yx}, is added to the interference generated by other nodes. Therefore, in such a network, interference for the desired $x-y$ link in HD and FD modes, assuming K is the same for all links, are as follows [24]:

$$I_{xy}^{HD} = \sum_{a\in\Phi_{HD}} PKh_{ay}l(a,y) + \sum_{a\in\Phi_{FD}} PK(h_{ay}l(a,y) + h_{m(a)y}l(m(a),y)) \quad (3)$$

$$I_{xy}^{FD} = \sum_{a\in\Phi_{HD}} PKh_{ay}l(a,y) + \sum_{a\in\Phi_{FD}} PK(h_{ay}l(a) + h_{m(a)y}l(m(a),y)) + P\beta \quad (4)$$

where Φ_{FD} and Φ_{HD} are the set of interferer nodes that are in FD and HD modes, respectively.

3 Hybrid duplex wireless network throughput

In this section, we discuss the optimization problem and choose the optimal mode for the desired network, using success probabilities and throughput. In addition, we compute the sub-optimal value for SIR threshold, when other parameters are fixed.

3.1 Throughput optimization using mode selection

As described in Section II, the success probability in such a system is defined as follows:

$$p_s \triangleq P_r(SIR_y > \theta) \quad (5)$$

wherein $P_r(.)$ denotes probability, θ is the SIR threshold and if the link between x and y operates in FD mode, $SIR_y = SIR_y^{FD}$ otherwise, $SIR_y = SIR_y^{HD}$.

The authors in [24] calculate success probabilities for a typical link under FD and HD conditions. Also, the authors have derived the throughput using these probabilities. The success probability under HD condition is given by [24]:

$$p_s^{HD} = \exp(-\lambda p_1 H(\theta R^\alpha, \alpha)) \exp(-\lambda p_2 F(\theta R^\alpha, \alpha, R)) \quad (6)$$

where $H(s,\alpha) \triangleq \frac{\pi^2 \delta s^\delta}{\sin(\pi\delta)}$ with $\delta = \frac{2}{\alpha}$ and

$$F(s,\alpha,R) \triangleq \int_0^\infty (2\pi - \frac{1}{1+sr^{-\alpha}} K(s,r,R,\alpha)) r dr \quad (7)$$

with $K(s,r,R,\alpha) = \int_0^{2\pi} \frac{d\varphi}{1+s(r^2+R^2+2rRcos\varphi)^{-\alpha/2}}$, and the success probability under FD condition is given by [24]: $p_s^{FD} = \kappa p_s^{HD}$ where $\kappa = e^{-\frac{\theta R^\alpha \beta}{K}}$. The

Table 1 List of parameters and variables used.

parameter	Meaning
$\hat{\Phi}$	IMPPP of node distribution with ground process Φ
p_1, p_2,p_3	Medium access probabilities for HD / FD / idle mode
$\lambda, \lambda_1, \lambda_2, \lambda_3$	Spatial density of network/ HD nodes / FD nodes / idle nodes
β	Residual self-interference-to-transmit power ratio
SIR_y^{HD}, SIR_y^{FD}	Signal-to-interference ratio of node y for HD /FD mode
$\tilde{\Phi}$	Set of transmitting nodes in a given time slot
P_{xy}	Transmit power from x to y
h_{xy}	Fading power coefficient with mean 1 from the desired transmitter x to y
Φ_{FD}, Φ_{HD}	Set of interferer FD / HD mode nodes
I_{xy}^{HD}, I_{xy}^{FD}	Interference conditional on that the link is in HD / FD mode
K	A constant that depends on the antenna characteristics and the average channel attenuations
G_{rx}, G_{tx}	Antenna gain at the receiver / transmitter
c_L	Speed of light
f_c	Carrier frequency of the signal
$l(x, y)$	Path loss function
α	Path loss exponent
θ	SIR threshold
p_s, p_s^{HD}, p_s^{FD}	Success probability, success probability provided that the link is in HD / FD mode
R	Distance of all links
T	Throughput
κ	Success probability coefficient for FD mode

unconditional success probability and throughput in such system are as follows [24]:

$$p_s = p_1 p_s^{HD} + p_2 p_s^{FD} \tag{8}$$

$$T \triangleq \lambda(p_1 p_s^{HD} + 2p_2 p_s^{FD}) \log(1+\theta) \tag{9}$$

In the following, we aim to obtain the local optimum densities for FD, HD and idle modes. We replace λp_i with λ_i for $i = \{1, 2, 3\}$ and define the optimization problem as follows:

$$\begin{aligned} &\max_{\lambda_1,\lambda_2} T = (\lambda_1 p_s^{HD} + 2\lambda_2 p_s^{FD}) \log(1+\theta) \\ &s.t. \quad \lambda_1 + \lambda_2 + \lambda_3 = \lambda \\ &\qquad \lambda_1 \geq 0 \\ &\qquad \lambda_2 \geq 0 \\ &\qquad \lambda_3 \geq 0 \end{aligned} \tag{10}$$

where $\lambda_1+\lambda_2+\lambda_3 = \lambda$ is the total density constraint and $\lambda_i \geq 0$ for $i = \{1, 2, 3\}$ satisfies the fact that density, is a non-negative number. Table 1 provides a description of system parameters.

Note that we calculate $F(\theta R^\alpha, \alpha, R)$ in (7) numerically. We use F and H instead of $F(\theta R^\alpha, \alpha, R)$ and $H(\theta R^\alpha, \alpha)$, respectively, for simplicity of notation. Due to the existence of an equality constraint and three inequality constraints in the optimization problem, we solve it based on the KKT conditions [34]. The following results are achieved in (11) wherein λ_1^{opt}, λ_2^{opt} and λ_3^{opt} are the local optimum value of λ_1, λ_2 and λ_3, respectively. The proof is presented in the Appendix.

Under the condition where no node is in HD mode, i.e., all nodes are in FD or idle modes, we have:

$$(\lambda_1, \lambda_2^{opt}, \lambda_3^{opt}) = \begin{cases} (0, \lambda, 0) & \text{if } \frac{1}{F} \geq \lambda \\ (0, \frac{1}{F}, \lambda - \frac{1}{F}) & \text{if } 0 < \frac{1}{F} < \lambda \end{cases} \tag{12}$$

Under the condition where no node is in FD mode, i.e., all nodes are in HD or idle modes, we have:

$$(\lambda_1^{opt}, \lambda_2, \lambda_3^{opt}) = \begin{cases} (\lambda, 0, 0) & \text{if } \frac{1}{H} \geq \lambda \\ (\frac{1}{H}, 0, \lambda - \frac{1}{H}) & \text{if } 0 < \frac{1}{H} < \lambda \end{cases} \tag{13}$$

3.2 Throughput optimization by calculating the value of sub-optimal SIR threshold

In this subsection, we solve the problem of maximizing the throughput by optimizing the SIR threshold value when the densities of FD, HD and idle nodes are determined. In this case, the calculated threshold value should satisfy the quality of service (QoS) for FD and HD devices. Therefore, the optimization problem is formulated as follows:

$$\begin{aligned} \max_{\theta} \quad & T = (\lambda_1 p_s^{HD} + 2\lambda_2 p_s^{FD}) \log(1+\theta) \\ s.t. \quad & \theta \geq \max\{SIR_{FD}^{QoS}, SIR_{HD}^{QoS}\} \end{aligned} \tag{14}$$

where, SIR_{FD}^{QoS} and SIR_{HD}^{QoS} are the minimum required SIR for FD and HD devices, respectively and the constraint $\theta \geq \max\{SIR_{FD}^{QoS}, SIR_{HD}^{QoS}\}$ guarantees QoS requirements in hybrid duplex mode. Note that if no node is in HD mode (i.e., $\lambda_1 = 0$) or no node is in FD mode (i.e., $\lambda_2 = 0$), the constraint in (14) is converted to the forms of $\theta \geq SIR_{FD}^{QoS}$ and $\theta \geq SIR_{HD}^{QoS}$, respectively.

Given the problem (14) where the throughput is a function of the integral $F(s, \alpha, R)|_{s=\theta R^\alpha}$, we find the sub-optimal value for θ. Therefore, we first compute the integral F at point $\theta = A = \max\{SIR_{FD}^{QoS}, SIR_{HD}^{QoS}\}$. Since the

---

$$(\lambda_1^{opt}, \lambda_2^{opt}, \lambda_3^{opt}) =$$

$$\begin{cases} (\lambda, 0, 0) & \text{if } \frac{1}{H} \geqslant \lambda \ \& \ 1 - \lambda H + \lambda F - 2K \geqslant 0 \\ (0, \lambda, 0) & \text{if } \frac{1}{F} \geqslant \lambda \ \& 2K - 2K\lambda(F-H) \geqslant 1 \\ (0, \frac{1}{F}, \lambda - \frac{1}{F}) & \text{if } 0 < \frac{1}{F} < \lambda \ \& \ 2KH \geqslant F \\ (\frac{1}{H}, 0, \lambda - \frac{1}{H}) & \text{if } 0 < \frac{1}{H} < \lambda \ \& \ 2KH \leqslant F \\ (\lambda - \frac{2K - \lambda F + \lambda H - 1}{H - F - 2KH + 2KF}, \frac{2K - \lambda F + \lambda H - 1}{H - F - 2KH + 2KF}, 0) & \text{if } z = \frac{2K - \lambda F + \lambda H - 1}{H - F - 2KH + 2KF} > 0 \ \& \\ & z < \lambda \ \& (\lambda - z)H + 2KHz \leqslant 1 \end{cases} \tag{11}$$

Algorithm 1 Proposed algorithm for sub-optimal SIR threshold

Require: ε, SIR_{FD}^{QoS}, SIR_{HD}^{QoS}.
Initialization
$k \leftarrow 1$, $\theta^k \leftarrow A = \max\{SIR_{FD}^{QoS}, SIR_{HD}^{QoS}\}$;
1: calculate F in term of θ^k;

Evaluate first point
2: **if** $\nabla T(\theta^k = A) \leqslant 0$ **then**
3: $\theta^{opt} = \theta^k$
4: **end if**

steepest descent method
5: **if** $\nabla T(\theta^k) > 0$ **then**
6: calculate F in term of θ^k;
7: calculate optimal λ (λ^*) using Golden section method;
8: $\theta^{k+1} \leftarrow \theta^k + \lambda^*(\nabla T(\theta^k))$;
9: **if** $\theta^{k+1} - \theta^k > \varepsilon$ **then**
10: $k \leftarrow k + 1$;
11: go to 6 line;
12: **else**
13: $\theta^{opt} = \theta^k$
14: **end if**
15: **end if**
16: **return** θ^{opt}

throughput is convex, if its gradient for this value of F at the point A is smaller than or equal to zero, then we have: $T^{\max} = T(\theta = A)$, otherwise, we can solve the problem using an iterative algorithm such as steepest descent method [34]. In this method, we have $\theta^{k+1} = \theta^k + \lambda^*(\nabla T(\theta^k))$ where θ^k is the current value of θ, k is the iteration index, λ^* is the optimal step value, $\nabla T(\theta^k)$ is the gradient of the throughput at the last point and θ^{k+1} is the new value calculated for θ. The λ^* value can be calculated, using line search methods such as the Golden Section method [34]. In the case of (14), we start with the point $\theta = A$, then we compute the value of F with this θ. Next, using the described method, we will get a step closer to the optimal value of θ. Then, we compute again the value of F with the new θ and repeat the above processes as far as $\theta^{k+1} \simeq \theta^k$, which is the optimal value of θ (i.e. θ^{opt}). The proposed algorithm is summarized in Algorithm 1. In our proposed Algorithm 1, the total computational cost can be summarized as the number of iterations of algorithm (N_{itter}) and the additional complexity of selecting the step size in the Golden section manner. The basic idea of the Golden Section line search is to use the same ratio named M in all iterations. Assuming that A and B are the desired length of final and first range of λ^*, therefore N as the smallest number of Golden Section's iterations is presented as $N_{step} = [\log_M^{(A/B)}]$ where $[(.)]$ denotes integer part and the total computational cost is given by $N_{step} * N_{itter}$.

Table 2 System Parameters

parameter	Meaning
Carrier frequency of the signal, f_c	2.4 GHz
Link density, λ	0.1
Path-loss exponent, α	4
Distance of all links, R	1 m
Residual self-interference-to-power ratio, β	0,1,10^{-4}
SIR threshold, θ	$-25 < \theta_{dB} < 20$

4 Numerical Results

In this section, we evaluate the proposed scheme by investigating the throughput of the considered system when local optimum densities for FD, HD and idle nodes are obtained, and also for the proposed Algorithm of determining the sub-optimal SIR threshold, using MATLAB software.

4.1 Throughput performance with mode selection

In this subsection, we compare the throughput of networks with HD-only, FD-only and the proposed method using numerical analysis. We show that the network throughput in the proposed mode selection design is higher compared to the scenarios when all active nodes are only in FD or HD modes. The parameter values for this subsection are given in Table 2.

Fig. 2(a), Fig. 3(a) and Fig. 4(a) depict the throughput performance conditioning on perfect SIC, no SIC and imperfect SIC, respectively and Fig. 2(b), Fig. 3(b) and Fig. 4(b) present the corresponding duplex mode densities. Note that legends of “T-opt- FD only”, “T-opt- HD only” and “T-opt-mode selection” in each of Fig. 2(a), Fig. 3(a) and Fig. 4(a) are related to the optimal throughput in the scenarios in which all the active nodes are in FD mode, all active nodes are in HD mode, and the state where nodes select their own mode using the proposed method, respectively. These graphs are calculated using (11), (12) and (13), respectively. Also, in Fig. 2(b), Fig. 3(b) and Fig. 4(b) the three top, bottom left and bottom right, depict the density of HD nodes, FD nodes, and the network nodes for three scenarios of all active nodes are in FD mode, all active nodes are in HD mode and active nodes are in hybrid mode, respectively. These graphs confirm the establishment of the problem (10) constraints.

From (9) we have: $T = (\lambda_1 p_s^{HD} + 2\lambda_2 p_s^{FD}) \log(1+\theta) = p'_s \times \log(1+\theta)$. As observed in Fig. 5 for small θ values, as θ increases, due to the high growth rate of $\log(1+\theta)$ compared to the decreasing rate of p'_s, the throughput that is the result of multiplication of these two expressions, increases. As θ exceeds a certain threshold (i.e., 3 dB), when the p'_s values are close to zero, the amount of throughput also reduces. In fact, when the SIR threshold is too

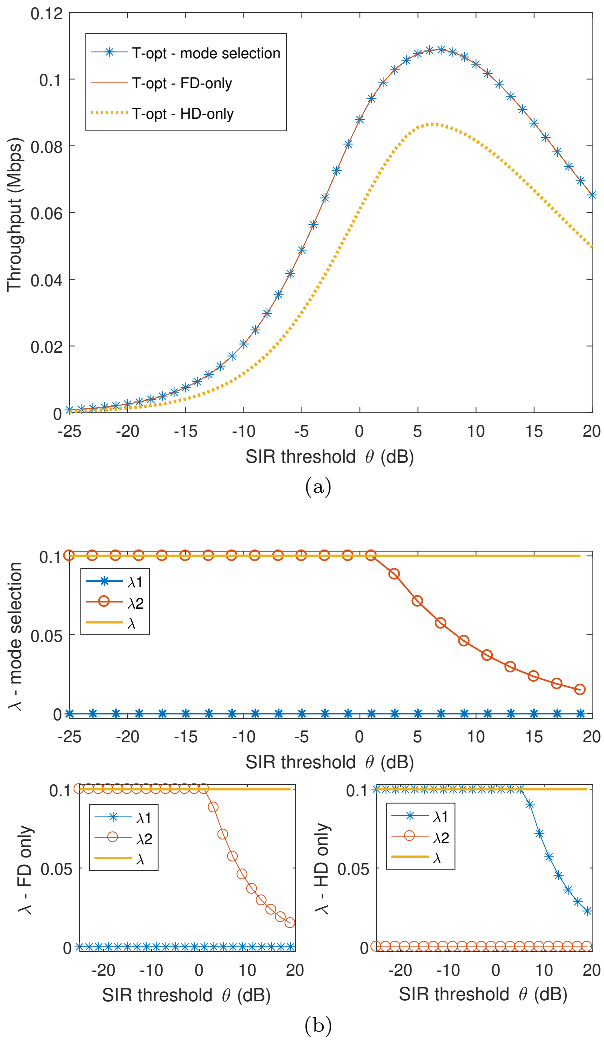

Fig. 2 (a) Throughput as a function of SIR threshold for $\beta = 0$ (perfect SIC). (b) densities of HD and FD nodes in proposed mode selection design, pure FD and pure HD scenarios for perfect SIC.

high, the number of links that satisfy the condition in (5) greatly reduces and consequently the throughput reduces as well.

Fig. 3(a) is plotted for no SIC condition, which shows that in this case the use of FD mode decreases the throughput due to the remainder of SI and as a consequence, the optimal mode selection is only between HD and idle modes, based on the network parameters.

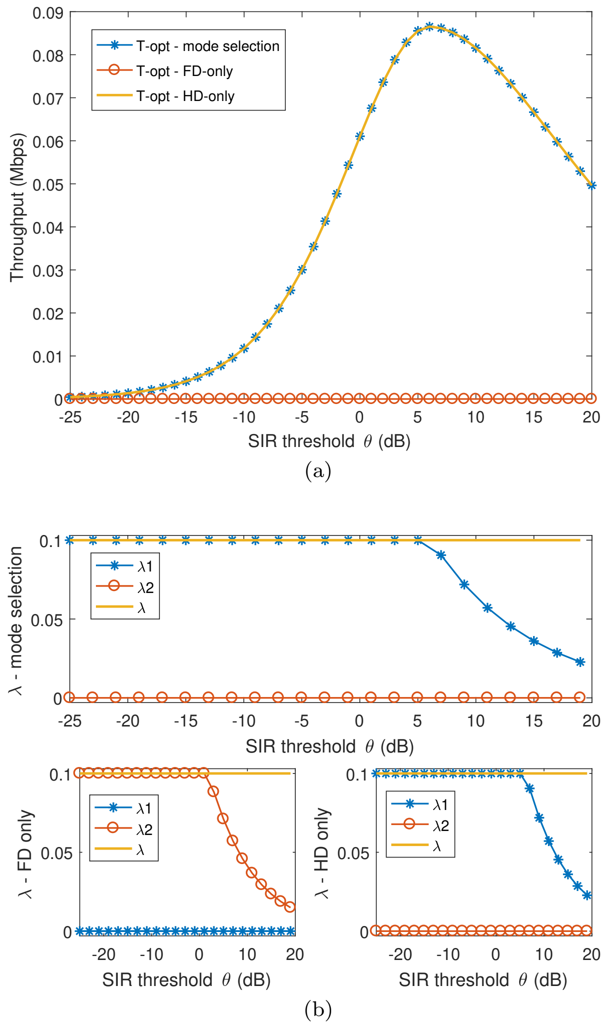

Fig. 3 (a) Throughput as a function of SIR threshold for $\beta = 1$ (no SIC). (b) densities of HD and FD nodes in proposed mode selection design, pure FD and pure HD scenarios for no SIC.

According to Fig. 2(a), when the SIC is perfect, putting all active nodes in FD mode, improves the system throughput and the curves corresponding to two scenarios of all active nodes in FD mode and the optimal mode selection, coincide. Therefore, as observed in Fig. 2(b), in order to increase the throughput, mode selection is applied only between FD and idle modes, based on the network parameters.

Fig. 4(a) depicts the necessity of selecting the optimal mode to improve the throughput. In this case that we have imperfect SIC, with respect to

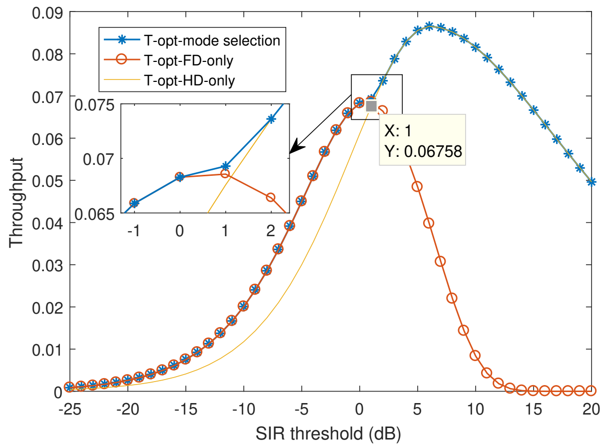

(a)

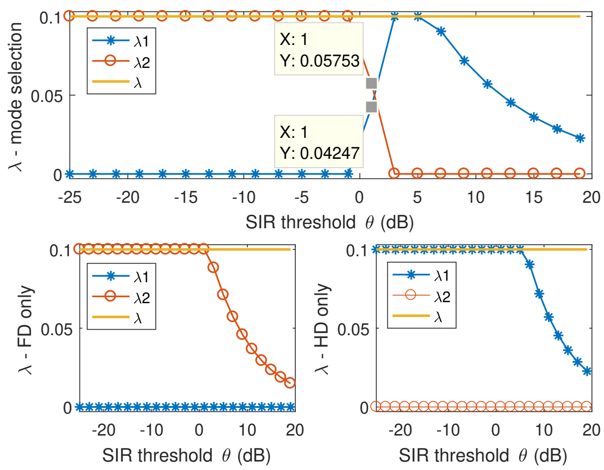

(b)

Fig. 4 (a) Throughput as a function of SIR threshold for $\beta = 10^{-4}$ (imperfect SIC). (b) densities of HD and FD nodes in proposed mode selection design, pure FD and pure HD scenarios for imperfect SIC.

the network parameters, somewhere in the interval 0 dB $< \theta <$ 5 dB, the throughput is greater than that of the case when all active nodes are in FD or HD modes, and in that range, some of the active nodes are in FD mode and some of them are in HD mode. By comparing Fig. 2(a), Fig. 3(a) and Fig. 4(a) and observing the peak of the throughput graph, the impact of imperfect SIC on the throughput can be observed.

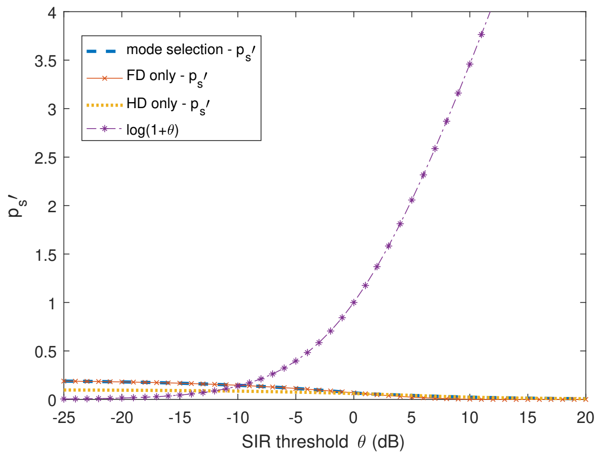

Fig. 5 p'_s for FD only, HD only and proposed mode selection network in compare with $\log(1+\theta)$.

4.2 Throughput performance with sub-optimal SIR threshold

In this subsection, we investigate the effect of optimizing the value of SIR threshold on the throughput, through numerical analysis. The parameter values for this subsection are given in Table 3.

Table 3 System Parameters

parameter	Meaning
Carrier frequency of the signal, f_c	2.4 GHz
Link density, λ	0.1
Path loss exponent, α	4
Distance of all links, R	1 m
Residual self-interference-to-power ratio, β	10^{-4}
λ_1	0.0425
λ_2	0.0575
SIR_{HD}^{QoS}	-1 dB
SIR_{FD}^{QoS}	0 dB

According to the results of the previous subsection, as we observe in Fig. 4(b), the calculated local optimum values of λ_1 and λ_2 for SIR threshold $\theta = 1$ dB, is equal to 0.0425 and 0.0575, respectively. Also according to Fig. 4(a) the value of the throughput corresponding to $\theta = 1$ dB is equal to 0.06758. In this subsection, we use these values of λ_1 and λ_2 and obtain their corresponding sub-optimal SIR threshold as $\theta = 1.8854$ dB and its corresponding throughput as $T^{\max} = 0.0701$ Mbps using the proposed Algorithm 1 and by using MATLAB for simulation. In addition, Fig. 6 shows the throughput curve as a function of SIR threshold, which is the result of an exhaustive search with a step of 0.1 for the density values shown in Table 3, using MATLAB. According to Fig. 6, the sub-optimal value of θ is approximately 1.9 dB and its corresponding throughput is 0.07009 Mbps. Therefore the throughput for optimized SIR threshold case is more than non-optimized one.

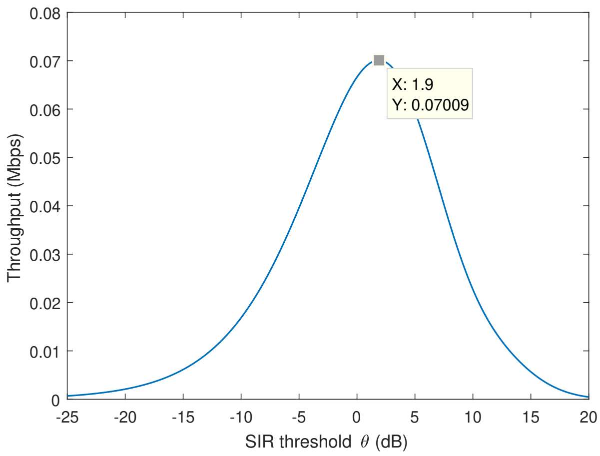

Fig. 6 Throughput in term of SIR threshold for $\beta = 10^{-4}$.

5 Conclusions

In this paper, mode selection problem in the mixed HD and FD wireless network was investigated, using stochastic geometry tool. It was shown that compared to HD mode, the SI in FD mode is an obstacle to improve the network throughput. Therefore, by choosing the optimum number of FD and HD devices in an imperfect SIC condition, we achieve higher throughput than pure FD or HD modes. We also improved the throughput via optimizing the SIR threshold value. In order to reduce the computational complexity, instead of joint optimization for throughput relative to densities and SIR threshold, we have optimized them separately. In fact, the value of the local optimum density of FD and HD nodes for a network can be calculated for a certain SIR threshold. Then, by placing those densities in the throughput equation, we have obtained the optimal SIR threshold value and achieve a higher throughput.

APPENDIX

In [34] the standard form of an optimization problem with equality and inequality constraints is defined as follows:

$$\begin{array}{lll} \min & f(x) & \\ s.t & g_j(x) \leqslant 0 & j = 1, 2, ..., m \\ & h_k = 0 & j = 1, 2, ..., m \end{array}$$

where f is the objective function, and g and h are the constraints of the problem. In this case, the KKT conditions can be written as follows:

$$\begin{array}{ll} \frac{\partial f}{\partial x_i} + \sum\limits_{j=1}^{m} \eta_j \frac{\partial g_j}{\partial x_i} + \sum\limits_{j=1}^{p} \mu_k \frac{\partial h_k}{\partial x_i} = 0, & i = 1, 2, \ldots, n \\ \eta_j g_j = 0, & j = 1, 2, \ldots, m \\ g_j \leqslant 0, & j = 1, 2, \ldots, m \\ \eta_j \geqslant 0, & j = 1, 2, \ldots, m \\ h_k\left(x\right) = 0, & k = 1, 2, \ldots, p \end{array}$$

where μ_k and η_k are the Lagrange coefficients. The optimization problem in (10), which has an equality constraint and three inequality constraints, can be described in the following standard form:

$$\begin{array}{l} \min f = -T \\ s.t.\ \lambda_1 + \lambda_2 + \lambda_3 = \lambda \\ \quad - \lambda_1 \leq 0 \\ \quad - \lambda_2 \leq 0 \\ \quad - \lambda_3 \leq 0 \end{array}$$

Applying the KKT conditions, leads to the following formulations:

$$\begin{bmatrix} -\log(1+\theta)\exp(-\lambda_1 H - \lambda_2 F)(1 - \lambda_1 H - 2KH\lambda_2) \\ -\log(1+\theta)\exp(-\lambda_1 H - \lambda_2 F)(-\lambda_1 F + 2K - 2KF\lambda_2) \\ 0 \end{bmatrix} + \begin{bmatrix} -1 & 0 & 0 \\ 0 & -1 & 0 \\ 0 & 0 & -1 \end{bmatrix} \begin{bmatrix} \eta_1 \\ \eta_2 \\ \eta_3 \end{bmatrix} + \mu \begin{bmatrix} 1 \\ 1 \\ 1 \end{bmatrix} = 0$$

where μ and η_i with $i \in \{1, 2, 3\}$ are Lagrange coefficients and K, H and F are obtained from the existing equations in section III. Therefore, we have:

$$A : -\log(1+\theta)\exp(-\lambda_1 H - \lambda_2 F)(1 - \lambda_1 H - 2KH\lambda_2) \quad -\eta_1 + \mu = 0$$
$$B : -\log(1+\theta)\exp(-\lambda_1 H - \lambda_2 F)(-\lambda_1 F + 2K - 2KF\lambda_2) \ -\eta_2 + \mu = 0$$
$$C : 0 - \eta_3 + \mu = 0 \rightarrow \eta_3 = \mu$$
$$D : \eta_1 \lambda_1 = 0$$
$$E : \eta_2 \lambda_2 = 0$$
$$F : \eta_3 \lambda_3 = 0$$
$$G : \lambda_i \geqslant 0, i = \{1, 2, 3\}$$
$$H : \sum_{i=1}^{3} \lambda_i = \lambda$$
$$I : \eta_i \geqslant 0, i = \{1, 2, 3\}$$

Given the equation G, each λ_i, $i \in \{1, 2, 3\}$ has two states: one is equal to zero and one to be positive. Therefore, there are eight modes to set them up (the whole-zero state is eliminated with respect to the relation H, and we have seven states):
Case 1: $\lambda_1 = 0, \lambda_2 = 0, \lambda_3 > 0 \Rightarrow \eta_3 = \mu = 0$
from A: $\eta_1 = -\log(1+\theta) \geqslant 0 \rightarrow \times$
from B: $\eta_2 = -2K\log(1+\theta) \geqslant 0 \rightarrow \times$

Case 2: $\lambda_1 = \lambda, \lambda_2 = 0, \lambda_3 = 0 \Rightarrow \eta_1 = 0$
from A: $\eta_3 = \mu = \log(1+\theta)\exp(-\lambda H)(1 - \lambda H) \geqslant 0 \rightarrow \lambda H < 1$
from B: $\eta_2 = \mu - \log(1+\theta)\exp(-\lambda H)(-\lambda F + 2K) \geqslant 0 \rightarrow 1 - \lambda H + \lambda F - 2K \geqslant 0$

Case 3: $\lambda_1 = 0, \lambda_2 = \lambda, \lambda_3 = 0 \Rightarrow \eta_2 = 0$
from B: $\eta_3 = \mu = \log(1+\theta)exp(-\lambda F)(2K - 2K\lambda F) \geqslant 0 \rightarrow \lambda F \leqslant 1$
from A: $\eta_1 = \log(1+\theta)exp(-\lambda F)(2K - 2K\lambda(F - H) - 1) \geqslant 0$
$\rightarrow 2K - 2K\lambda(F - H) \geqslant 1$

Case 4: $\lambda_1 = 0, \lambda_2 > 0, \lambda_3 > 0 \Rightarrow \eta_2 = 0, \eta_3 = \mu = 0$
from B: $2K - 2KF\lambda_2 = 0 \rightarrow \lambda_2 = \frac{1}{F} > 0$
from H:$\lambda_3 = \lambda - \frac{1}{F} > 0 \rightarrow \frac{1}{F} < \lambda$
from A:$\eta_1 = 0 - \log(1+\theta)exp(-1)(1 - 2K\frac{H}{F}) \geqslant 0 \rightarrow F \leqslant 2KH$

Case 5: $\lambda_1 > 0, \lambda_2 = 0, \lambda_3 > 0 \Rightarrow \eta_1 = 0, \eta_3 = \mu = 0$
from A: $1 - \lambda_1 H = 0 \rightarrow \lambda_1 = \frac{1}{H} > 0$
from H: $\lambda_3 = \lambda - \frac{1}{H} > 0 \rightarrow \frac{1}{H} < \lambda$
from B: $\eta_2 = 0 - \log(1+\theta)exp(-1)(-\frac{F}{H} + 2K) \geqslant 0 \rightarrow F \geqslant 2KH$

Case 6: $\lambda_1 > 0, \lambda_2 > 0, \lambda_3 = 0 \Rightarrow \eta_1 = 0, \eta_2 = 0$

from A,B,H: $\begin{cases} \lambda_1 = \lambda - \frac{2K-\lambda F+\lambda H-1}{H-F-2KH+2KF} > 0 \\ \lambda_2 = \frac{2K-\lambda F+\lambda H-1}{H-F-2KH+2KF} > 0 \end{cases}$

from A:$\eta_3 = \mu \geqslant 0 \rightarrow \lambda_1 H + 2KH\lambda_2 \leqslant 1$

Case 7: $\lambda_1 > 0, \lambda_2 > 0, \lambda_3 > 0 \Rightarrow \eta_1 = 0, \eta_2 = 0, \eta_3 = \mu = 0$
from A,B: $\begin{cases} 1 - \lambda_1 H - 2KH\lambda_2 = 0 \\ -\lambda_1 F + 2K - 2KF\lambda_2 = 0 \end{cases}$
$\rightarrow F = 2KH$ for $\forall \underset{i=1,2,3}{\lambda_i} > 0$ & $\lambda_1 + \lambda_2 + \lambda_3 = \lambda$

References

1. Li R, Chen Y, Li GY, Liu G (2017) Full-duplex cellular networks. IEEE Communications Magazine 55(4):184–191, DOI 10.1109/MCOM.2017.1600361CM
2. Naslcheraghi M, Ghorashi SA, Shikh-Bahaei M (2017) Full-duplex device-to-device collaboration for low-latency wireless video distribution. In: 2017 24th International Conference on Telecommunications (ICT), pp 1–5, DOI 10.1109/ICT.2017.7998228
3. Zhang Z, Long K, Vasilakos AV, Hanzo L (2016) Full-duplex wireless communications: Challenges, solutions, and future research directions. Proceedings of the IEEE 104(7):1369–1409, DOI 10.1109/JPROC.2015.2497203
4. Naslcheraghi M, Ghorashi SA, Shikh-Bahaei M (2017) Fd device-to-device communication for wireless video distribution. IET Communications 11(7):1074–1081, DOI 10.1049/iet-com.2016.0675
5. Sharma SK, Bogale TE, Le LB, Chatzinotas S, Wang X, Ottersten B (2018) Dynamic spectrum sharing in 5g wireless networks with full-duplex technology: Recent advances and research challenges. IEEE Communications Surveys Tutorials 20(1):674–707, DOI 10.1109/COMST.2017.2773628
6. Ernest TZH, Madhukumar AS, Sirigina RP, Krishna AK (2019) Outage analysis and finite snr diversity-multiplexing tradeoff of hybrid-duplex systems for aeronautical communications. IEEE Transactions on Wireless Communications 18(4):2299–2313, DOI 10.1109/TWC.2019.2902550
7. Wei Z, Sun S, Zhu X, Huang Y, Wang J (2018) Energy-efficient hybrid duplexing strategy for bidirectional distributed antenna systems. IEEE Transactions on Vehicular Technology 67(6):5096–5110, DOI 10.1109/TVT.2018.2814047
8. Ernest TZH, Madhukumar AS, Sirigina RP, Krishna AK (2019) A hybrid-duplex system with joint detection for interference-limited uav communications. IEEE Transactions on Vehicular Technology 68(1):335–348, DOI 10.1109/TVT.2018.2878889
9. Naslcheraghi M, Ghorashi SA, Shikh-Bahaei M (2017) Performance analysis of inband fd-d2d communications with imperfect si cancella-

tion for wireless video distribution. In: 2017 8th International Conference on the Network of the Future (NOF), pp 176–181, DOI 10.1109/NOF.2017.8251246

10. Cao Y, Zhao N, Pan G, Chen Y, Fan L, Jin M, Alouini M (2019) Secrecy analysis for cooperative noma networks with multi-antenna full-duplex relay. IEEE Transactions on Communications 67(8):5574–5587, DOI 10.1109/TCOMM.2019.2914210
11. Chen B, Chen Y, Chen Y, Cao Y, Ding Z, Zhao N, Wang X (2019) Secure primary transmission assisted by a secondary full-duplex noma relay. IEEE Transactions on Vehicular Technology 68(7):7214–7219, DOI 10.1109/TVT.2019.2919873
12. Wang K, Yu FR, Wang L, Li J, Zhao N, Guan Q, Li B, Wu Q (2019) Interference alignment with adaptive power allocation in full-duplex-enabled small cell networks. IEEE Transactions on Vehicular Technology 68(3):3010–3015, DOI 10.1109/TVT.2019.2891675
13. Gaber A, Youssef E, Rizk MRM, Salman M, Seddik KG (2020) Cooperative delay-constrained cognitive radio networks: Delay-throughput trade-off with relaying full-duplex capability. IEEE Access pp 1–1, DOI 10.1109/ACCESS.2020.2964565
14. Wang X, Huang H, Hwang T (2016) On the capacity gain from full duplex communications in a large scale wireless network. IEEE Transactions on Mobile Computing 15(9):2290–2303, DOI 10.1109/TMC.2015.2492544
15. Haenggi M (2012) Stochastic geometry for wireless networks. Cambridge University Press
16. Tang W, Feng S, Liu Y, Ding Y (2016) Hybrid duplex switching in heterogeneous networks. IEEE Transactions on Wireless Communications 15(11):7419–7431, DOI 10.1109/TWC.2016.2602329
17. Thanh PD, Hoan TNK, Koo I (2019) Joint resource allocation and transmission mode selection using a pomdp-based hybrid half-duplex/full-duplex scheme for secrecy rate maximization in multi-channel cognitive radio networks. IEEE Sensors Journal pp 1–1, DOI 10.1109/JSEN.2019.2958966
18. Liu J, Han S, Liu W, Yang C (2017) The value of full-duplex for cellular networks: A hybrid duplex-based study. IEEE Transactions on Communications 65(12):5559–5573, DOI 10.1109/TCOMM.2017.2743689
19. Li S, Zhou M, Wu J, Song L, Li Y, Li H (2017) On the performance of x-duplex relaying. IEEE Transactions on Wireless Communications 16(3):1868–1880, DOI 10.1109/TWC.2017.2656887
20. Kwon T, Lee H (2018) Hybrid duplex wireless peer discovery with imperfect self-interference cancellation. IEEE Communications Letters 22(3):598–601, DOI 10.1109/LCOMM.2017.2780095
21. Otyakmaz A, Schoenen R, Dreier S, Walke BH (2008) Parallel operation of half- and full-duplex fdd in future multi-hop mobile radio networks. In: 2008 14th European Wireless Conference, pp 1–7, DOI 10.1109/EW.2008.4623892

22. Yamamoto K, Haneda K, Murata H, Yoshida S (2011) Optimal transmission scheduling for a hybrid of full- and half-duplex relaying. IEEE Communications Letters 15(3):305–307, DOI 10.1109/LCOMM.2011.011811.101925
23. Lee J, Quek TQS (2015) Hybrid full-/half-duplex system analysis in heterogeneous wireless networks. IEEE Transactions on Wireless Communications 14(5):2883–2895, DOI 10.1109/TWC.2015.2396066
24. Tong Z, Haenggi M (2015) Throughput analysis for full-duplex wireless networks with imperfect self-interference cancellation. IEEE Transactions on Communications 63(11):4490–4500, DOI 10.1109/TCOMM.2015.2465903
25. Hemachandra KT, Fapojuwo AO (2017) Distance based duplex mode selection in large scale peer-to-peer wireless networks. In: 2017 IEEE International Conference on Communications (ICC), pp 1–6, DOI 10.1109/ICC.2017.7996444
26. Yao Y, Li B, Li C, Yang C, Xia B (2020) Downlink performance analysis of the full-duplex networks with interference cancellation. IEEE Transactions on Communications pp 1–1, DOI 10.1109/TCOMM.2020.2965536
27. Zheng T, Wang H, Yuan J, Han Z, Lee MH (2017) Physical layer security in wireless ad hoc networks under a hybrid full-/half-duplex receiver deployment strategy. IEEE Transactions on Wireless Communications 16(6):3827–3839, DOI 10.1109/TWC.2017.2689005
28. Li Y, Wang T, Zhao Z, Peng M, Wang W (2015) Relay mode selection and power allocation for hybrid one-way/two-way half-duplex/full-duplex relaying. IEEE Communications Letters 19(7):1217–1220, DOI 10.1109/LCOMM.2015.2433260
29. Fang Z, Ni W, Liang F, Shao P, Wu Y (2017) Massive mimo for full-duplex cellular two-way relay network: A spectral efficiency study. IEEE Access 5:23288–23298, DOI 10.1109/ACCESS.2017.2766079
30. Gazestani AH, Ghorashi SA, Mousavinasab B, Shikh-Bahaei M (2019) A survey on implementation and applications of full duplex wireless communications. Physical Communication 34:121–134, DOI 10.1016/j.phycom.2019.03.006
31. Towhidlou V, Shikh-Bahaei M (2019) Full-duplex d2d communications in vehicular networks. In: 2019 IEEE Wireless Communications and Networking Conference (WCNC), pp 1–6, DOI 10.1109/WCNC.2019.8885733
32. Ernest TZH, Madhukumar AS, Sirigina RP, Krishna AK (2018) Hybrid-duplex systems for uav communications under rician shadowed fading. In: 2018 IEEE 88th Vehicular Technology Conference (VTC-Fall), pp 1–5, DOI 10.1109/VTCFall.2018.8690623
33. Cheng W, Zhang W, Liang L, Zhang H (2019) Full-duplex for multi-channel cognitive radio ad hoc networks. IEEE Network 33(2):118–124, DOI 10.1109/MNET.2018.1700401
34. bakr M (2013) Nonlinear optimization in electrical engineering with applications in MATLAB, London. The Institution of Engineering and Technology